

**Title:**

TMEM184B controls pruriceptor specification and function

**Authors:**

Erik G. Larsen<sup>1</sup>, Tiffany S. Cho<sup>1</sup>, Matthew L. McBride<sup>1</sup>, Jing Feng<sup>2</sup>, Bhagyashree Manivannan<sup>1</sup>,  
Cynthia Madura<sup>3</sup>, Nathaniel E. Klein<sup>1</sup>, Elizabeth B. Wright<sup>1</sup>, Hector D. Garcia-Verdugo<sup>1</sup>, Chelsea  
Jarvis<sup>1</sup>, Rajesh Khanna<sup>3</sup>, Hongzhen Hu<sup>2</sup>, Tally M. Largent-Milnes<sup>3</sup>, and Martha R.C.  
Bhattacharya\*<sup>1</sup>

**Affiliations:**

<sup>1</sup> Department of Neuroscience, University of Arizona, 1040 E 4<sup>th</sup> Street, Tucson AZ 85721

<sup>2</sup> Center for the Study of Itch and Sensory Disorders, Department of Anesthesiology,  
Washington University School of Medicine, 660 Euclid Avenue, St. Louis MO 63110

<sup>3</sup> Department of Pharmacology, University of Arizona College of Medicine, 1501 N. Campbell  
Avenue, Tucson AZ 85724

**Correspondance:** marthab1@email.arizona.edu

## Summary

Nociceptive and pruriceptive neurons in the dorsal root ganglia (DRG) convey sensations of pain and itch to the spinal cord, respectively. A sub-population of these neurons, marked by Somatostatin (*Sst*) expression, is responsible for detecting the cytokine IL-31, a mediator of acute itch and atopic dermatitis. The mechanisms responsible for specifying this population are largely unknown. Here we show that *Tmem184b*, a gene with known roles in axon degeneration and nerve terminal maintenance, is required for the expression of a substantial cohort of receptors, including IL31RA, that mediate acute itch. Mice lacking *Tmem184b* fail to respond to IL-31, but maintain normal responses to pain and mechanical force, suggesting a specific defect in pruriception. The number of *Sst*<sup>+</sup> neurons is reduced in *Tmem184b*-mutant mice, indicating a likely defect in neuron subtype specification. Rescue experiments in adults versus embryonic neurons support a primary role for TMEM184B during development. We evaluated DRG gene expression across embryonic and early postnatal development and found that levels of Wnt signaling components are significantly reduced in embryonic DRG from *Tmem184b*-mutants and restored upon re-expression of *Tmem184b*. In summary, we have identified a mechanism controlled by TMEM184B that gates proper specification of pruriceptive neurons in the DRG through control of Wnt signaling. TMEM184B is thus critical for proper pruriceptive development and adult somatosensation.

## Introduction

Somatosensory neurons transduce multiple types of stimuli, including temperature, chemical, and physical changes in the local environment of their nerve endings. Nerve endings receiving these cues can also directly sense inflammatory compounds, and this inflammation alters their response properties to cause hyperalgesia (heightened responses to noxious stimuli) and allodynia (painful responses to non-noxious stimuli). A common consequence of increased skin inflammation is the triggering of itch.

Acute and chronic itch are significant morbidities in humans. Itch-causing pathological conditions have a variety of causes, including skin disorders (atopic dermatitis), drug-induced reactions, systemic disorders such as liver disease, and other neurological disorders (Dong and Dong, 2018). The sensation of itch is distinct from pain and is carried by a subset of itch-specific somatosensory neurons called pruriceptive neurons with cell bodies in the dorsal root ganglia (DRG). Skin itch is triggered by release of pro-inflammatory compounds such as cytokines (IL-4, IL-13, and IL-31), thymic stromal lymphopoietin (TSLP), and histamine from mast cells and epithelial cells, which act upon membrane receptors and channels present in epidermal nerve endings (Oetjen et al., 2017; Solinski et al., 2019; Wilson et al., 2013). In addition to chemical itch, mechanical stimuli can evoke similar itch sensations but rely on a distinct spinal circuit (Acton et al., 2019; Bourane et al., 2015; Pagani et al., 2019; Pan et al., 2019).

Somatosensory neurons have been classically categorized using soma size, electrical properties (including myelination state), and expression of a few markers that include lectins (IB4), neuroactive peptides, and ion channels. Recently, multiple groups have described the diversity of somatosensory neurons from the adult DRG using single-cell RNA sequencing, a powerful approach that has allowed an improved classification of subtypes of sensory neurons and their abilities to respond to agonists (Li et al., 2016a; Usoskin et al., 2015). These studies have classified DRG neurons into six to eight defined groups based solely on expression of unique transduction or signaling molecules. In addition, by genetically labeling and sorting DRG

populations prior to RNAseq, the ion channels conferring unique electrical properties have been mapped to eight distinct populations (Zheng et al., 2019).

One population of DRG neurons identified in these single cell RNAseq studies is uniquely identified by expression of the peptides *Nppb* (natriuretic peptide B, also called brain natriuretic peptide, or BNP) and Somatostatin (*Sst*), as well as IL-31 receptor type a (*Il31ra*) (Li et al., 2016a; Usoskin et al., 2015). These cells, representing 6-8% of all neurons in the DRG, are purely pruriceptive, transmitting itch, but not pain, signals to the dorsal horn of the spinal cord. (Huang et al., 2018) These neurons develop from an initially *Runx1*<sup>+</sup>, *TrkA*<sup>+</sup> population that ultimately loses *TrkA* expression but gains peptidergic markers such as Calcitonin gene related peptide (CGRP) (Lallemend and Ernfors, 2012). How this subset is specified remains a mystery.

TMEM184B is a relatively uncharacterized 7-pass transmembrane protein that is a member of the Transporter-Opin-GPCR (TOG) superfamily of proteins (Yee et al., 2013). TMEM184B is required for efficient axon degeneration following nerve injury, and also for proper sensory and motor nerve terminal maintenance (Bhattacharya et al., 2016). In mice lacking *Tmem184b*, nociceptive terminals in the epidermis show swollen endings, and mice show deficits in broad measures of sensorimotor behavior (Bhattacharya et al., 2016). Here we show that TMEM184B controls the expression of a large cohort of sensory receptors in the DRG, specifically those in the NP3/C2 population mediating pruriception. We found specific behavioral defects in acute itch, but not pain, when *Tmem184b* is absent, showing that TMEM184B is required for proper pruriception. *Tmem184b* loss causes a reduction in the total number of NP3/C2 neurons in adults. TMEM184B is also required for expression of critical drivers of sensory neurogenesis in embryos, suggesting an early role for TMEM184B in sensory development. Rescue experiments in both adults and embryos support a primary role for TMEM184B in pruriceptive neuron specification through control of Wnt signaling. Our data identify a critical role for TMEM184B in the establishment of the neurons responsible for primary pruriception.

## Results

### TMEM184B Controls the Expression of Pruriceptive Markers

In studying the nervous system phenotypes of loss of the transmembrane protein, TMEM184B, which include axon protection as well as dysmorphic nerve terminals (Bhattacharya et al., 2016), we sought to identify expression changes that could contribute to these phenotypes. We performed RNA sequencing on isolated adult DRGs of 6-month-old *Tmem184b* global knockout mice and compared sequences to age-matched wild-type mice. We observed 316 genes with significantly downregulated (FDR  $\leq$  0.05) transcript expression in *Tmem184b*-mutant ganglia, and 90 genes that had significantly upregulated transcripts (Figure 1A-B). Strikingly, the downregulated genes contained a large fraction of markers previously identified in single-cell RNAseq studies as being unique to a population of pruriceptive neurons (called C2 or NP3 in previous studies) (Chiu et al., 2014; Li et al., 2016b). The key markers of NP3/C2 neurons are dramatically downregulated, with *Ii31ra*, *Nppb*, and *Sst* being among the largest changes seen in the dataset (Figure 1B). However, other types of neurons also showed decreased expression of their unique markers, including NP2/C4 (identified by *Mrgpra3*) and NP1/C5-6 (identified by *Mrgprd*) (Figure 1C). Taken together, this data identifies TMEM184B as a major regulator of somatosensory gene expression, particularly in pruriceptive populations.

To predict the functional significance of these expression changes, we performed pathway analysis (see methods for details). Downregulated transcripts were enriched in pathways such as GPCR signaling, mitogen-activated protein (MAP) kinase signaling, and synaptic transmission (Figure 1D). When human phenotype ontology was examined, pruritus was the top and most significantly changed feature ( $p < 0.003$ ). These data show that TMEM184B is required for appropriate transcription of signaling pathways critical to normal sensory function.

### TMEM184B is required for itch, but not pain, responses

To test the behavioral consequences of the expression changes observed in *Tmem184b*-mutant mice, we challenged them with agonists that promote itch or pain. The cytokine IL-31, implicated in atopic dermatitis, activates the IL31RA/OSMR heterodimeric receptor on NP3/C2 DRG neurons, whereas the anti-malarial agent chloroquine (CQ) activates MRGPRA3 on NP2/C4 DRG neurons (Cevikbas et al., 2014; Dillon et al., 2004; Liu et al., 2009). *Tmem184b*-mutant mice are resistant to scratching evoked by IL-31 injection (Figure 2A). In addition, mutant mice have a reduced response to chloroquine, although the reduction does not reach statistical significance (Figure 2B,  $p = 0.07$ ). To examine the effects on other nociceptive populations, we performed mechanical threshold and thermal pain testing. *Tmem184b*-mutant mice responded normally to these stimuli (Figure 2C-E). Taken together, this data shows that TMEM184B is selectively required for behavioral responses to pruriceptive agonists.

### **TMEM184B is required for proper NP3/C2 development**

One possible explanation for the reduction in NP3/C2-associated transcripts is that NP3/C2 neurons failed to develop. Because NP3/C2 DRG neurons are uniquely marked by *Sst* expression, we used a genetic strategy to label these markers using *Sst*<sup>Cre</sup> combined with Cre-dependent tdTomato expression. We find that the percent of adult neurons labeled with tdTomato is reduced but not completely eliminated in *Tmem184b*-mutant mice (Figure 3A-B). Thus, some loss of these neurons may contribute to the reduction of gene expression seen in RNAseq experiments.

One possibility we considered is that the *Sst* promoter may have briefly turned on during earlier time points, and then failed to be maintained in adults (*Sst* transcript levels are 27% of wild-type in adult DRGs). To interrogate whether somatosensory neuron developmental specification had been altered, we used RNA sequencing to examine the onset of pruriceptive neuron markers at different developmental stages: embryonic day 13.5, postnatal day 0, and postnatal day 10. At the latest time point, expression of NP3/C2 DRG markers has been previously observed (Lallemend and Ernfors, 2012). We found expression of *Tmem184b* by

E13.5 (Figure 3C) and continuing throughout DRG differentiation; this is also supported by a recently published single-cell RNAseq timecourse analysis showing *Tmem184b* expression in sensory neuron progenitors as early as E11.5 (Sharma et al., 2020). *Sst* expression in wild-type began at P0 and was maintained at high levels through P10, when NP3/C2 neurons express the majority of their unique markers (Figure 3D). In *Tmem184b*-mutant mice, *Sst* failed to turn on at P0 but had a burst of expression at P10. This burst of *Sst* activity in mutants at P10 likely causes tdTomato expression, as these neurons would be permanently marked following the burst even if they express little *Sst* as adults. In comparison, *Il31ra* expression is suppressed throughout these developmental timepoints (Figure 3E), while *Nppb* expression is unaffected prior to adulthood (Figure 3F). This data argues for a functional loss of C2 neurons in *Tmem184b*-mutant mice. Supporting this interpretation, we see significant reductions at E13.5 in neurogenin 1 (*Neurog1*), neurogenin 2 (*Neurog2*), and POU domain, class 4, transcription factor 1, (*Pou4f1*, also known as *Brn3a*) (Figure 3G-I). These transcription factors are critical in establishing neuronal numbers and identity in migrating neural crest progenitors (Lallemend and Ernfors, 2012; Lee et al., 2004; Raisa Eng et al., 2001). Many other genes necessary for somatosensory development or mature function are also dysregulated (Figure S1). Taken together, our data supports a model in which TMEM184B, acting early in neuronal development, controls a developmental program leading to the proper specification of pruriceptive neurons.

### **Aberrant cellular responses to nociceptive and pruriceptive agonists in *Tmem184b*-mutant mice**

To determine whether functional shifts in adult somatosensory neuron populations had occurred, we performed calcium imaging on dissociated adult DRG neurons. We saw significant reductions in the percentage of neurons that responded to the broad nociceptive receptor agonists, capsaicin (a TRPV1 agonist) and allyl isothiocyanate (AITC, a TRPA1 agonist) (Figure 4A-B). The percent of neurons responding to two agonists specific for the NP3/C2 population, CYM5442 (an S1PR1 agonist) and LY344862 (an HTR1F agonist) was reduced (Figure 4D-E).

These results support our genetic labeling data and suggest that cell loss contributes to our prurceptive phenotypes. Paradoxically, mutant mice showed an increased percentage of neurons responding to both IL-31 and chloroquine (Figure 4F-G). Because in wild type mice, *S1pr1*, *Htr1f*, and *Il31ra* are all unique markers of NP3/C2 neurons, we interpret these dynamic changes as evidence that gene expression has been at least partially uncoupled with cell fate in *Tmem184b*-mutant ganglia. To rectify the increase in the percentage of IL-31 responsive neurons with the loss of behavioral responses, we evaluated the amplitude of IL-31-induced calcium increases in individual neurons. Among neurons classified as responders, IL-31 triggered substantially weaker responses in mutant neurons when compared to wild type (Figure 4H). The reduction in responses of individual neurons to IL-31 likely contributes to the loss of IL-31-induced pruriception in adults.

#### ***In vivo* re-expression of *Tmem184b* in adult mutant ganglia does not increase IL-31 responses**

Given our results showing reductions in the NP3/C2 population, we sought to evaluate whether TMEM184B contributes solely to early neuronal specification or if it can influence prurceptive function in adulthood. If TMEM184B's role is primarily developmental, then re-expression in adults should not rescue IL-31 responsiveness. We constructed an adeno-associated (AAV9) virus encoding *Tmem184b* under the control of the neuronal-specific Synapsin promoter, and injected this virus, or control AAV9 expressing only mCherry, into the cervical intrathecal space (Figure 5A). Histological analysis showed that virus was able to spread to DRG from C1-C10 (Figure 5B) and also into some of the central axonal projections of these DRGs into the dorsal horn (Figure 5C). Virus expression was also seen in the dorsal gray matter (Figure 5C). In these mice, we evaluated scratching responses to subsequent IL-31 injection. All IL-31-injected mutant mice showed some scratching responses compared to saline controls, suggesting that AAV injection and expression influenced the baseline levels of IL-31 responsiveness (Figure 5D). Surprisingly, we found that in wild-type mice, overexpression of



*Tmem184b* attenuates scratching to IL-31 injection. However, we were unable to alter mutant responsiveness with adult re-expression of *Tmem184b*. The failure to rescue in adults is consistent with a primary effect of TMEM184B activity during development of pruriceptive neurons.

### **TMEM184B controls expression of Wnt signaling components in embryonic DRG neurons**

Given our data indicating a reduction in pruriceptive neurons and significant decreases in the expression of critical transcription factors required for sensory differentiation, we sought to determine the molecular mechanism responsible for these effects. We cultured E13.5 embryonic DRG neurons from wild type or mutant mice for 14 days (DIV 14, roughly equivalent timewise to postnatal day 8) (Figure 6A). In a subset of neurons from each mutant embryo, we re-expressed *Tmem184b* using lentiviral transduction on the day of dissociation. At day 14, we collected RNA and performed RNA sequencing for each condition. We identified differentially expressed genes in DIV 14 mutant neurons relative to wild type (Figure 6B), and in mutant neurons with and without restoration of *Tmem184b* (Figure 6C). Within these genes, we identified those that both decreased in the absence of *Tmem184b* and were increased in mutants upon re-expression of *Tmem184b*. Our analysis resulted in the identification of 304 genes matching this pattern. Gene ontology analysis revealed biological processes significantly over-represented by these genes, representing processes positively regulated by TMEM184B activity. Genes negatively regulated by TMEM184B were also identified and analyzed, though there were fewer in this group (Figure S2). The most over-represented process among genes positively regulated by TMEM184B is the planar cell polarity (PCP) pathway (23.5-fold enriched), a non-canonical Wnt signaling pathway. Canonical Wnt signaling was also enriched (7.93-fold). Both groups contain multiple Wnt receptors including Frizzled-1, Frizzled-2, and Frizzled-10. Many of the processes controlled by TMEM184B influence important neuronal functions including calcium regulation (7.86-fold enrichment) and axon guidance (4.18-fold

enrichment). This data implicates TMEM184B in controlling key developmental steps in the establishment of the somatosensory system. Wnt signaling is known to control the early expression of Neurogenins and *Brn3a* during sensory neuron differentiation (Kondo et al., 2011). Our data therefore support a model in which TMEM184B controls the proper expression of Wnt signaling components necessary for the cascade of developmental events leading to pruriceptive neuron differentiation.

## Discussion

Our data support a significant role for TMEM184B in the control of pruriception. *Tmem184b*-mutant DRGs show reduction of pruriceptor transcripts in the NP3/C2 population. Of note, mRNA expression of the IL-31 receptor subunit, *Il31ra*, and its co-receptor, *Osmr*, are both strongly decreased in the absence of *Tmem184b*. We see reduced IL-31-induced scratching as well as lower response magnitudes in individual neurons in response to IL-31 application in mutant mice. IL-31-mediated itch is central to the development of atopic dermatitis, and thus the expression and function of its receptor is of significant medical interest (Dillon et al., 2004). Our data identify a novel mechanism promoting the expression of the IL-31 receptor on sensory neurons and ultimately controlling IL-31 induced behaviors.

Using a genetic labeling strategy, we found that NP3/C2 neuron numbers are reduced in the absence of *Tmem184b*, though they are not completely eliminated. Using calcium imaging, we found a reduction of nociceptive neurons generally and skewed numbers and/or sensitivity of remaining pruriceptive populations. In addition, at E13, we see reductions in transcripts encoding critical developmental factors including *Neurog1*, *Neurog2*, and *Pou4f1*. These three factors are essential for the establishment and differentiation of neurons within sensory ganglia (Lallemend and Ernfors, 2012). Based on this evidence, we believe that TMEM184B acts early in sensory development to promote the proper specification of nociceptive and pruriceptive neurons.

Our *Tmem184b*-mutant phenotypes are consistent with an effect on sensory neuron differentiation. How TMEM184B activity directly controls these developmental programs is still mysterious. Data from embryonic neurons indicate that *Tmem184b* positively regulates components of Wnt signaling. Wnt signaling is critical for early neural crest development, and in stem cells, Wnt signaling induces *Neurog1* and *Pou4f1* expression (Garcia-Morales et al., 2009; Kondo et al., 2011; Lee et al., 2004). One way this might occur is through Wnt activation of transcription via the homeodomain transcription factor, *Tlx3*. Supporting this idea, *Tlx3* nociceptor-specific knockouts show loss of pruriceptive populations as well as reductions in the same pruriceptive markers as in *Tmem184b*-mutant DRGs (Huang et al., 2017; Lopes et al., 2012). Intriguingly, the effect of blockade of Wnt secretion on the morphology of the mouse neuromuscular junction is strikingly similar to that seen in *Tmem184b*-mutant mice, further implicating a link between TMEM184B and Wnt signaling (Bhattacharya et al., 2016; Shen et al., 2018). Future experiments should test how TMEM184B activity and appropriate Wnt signaling in early sensory development are associated.

It is possible that TMEM184B plays an additional role in adult nociceptor maintenance. First, in wild type mice, over-expression of *Tmem184b* causes reduction in IL-31-induced scratching (Figure 5D). One possible explanation is that TMEM184B may be promoting apoptosis. In support of this model, we see decreased expression of apoptotic pathway components when *Tmem184b* is absent and restoration of these components upon *Tmem184b* re-expression in cultured DRGs (data not shown). Future experiments deleting *Tmem184b* solely in adults would be necessary to clarify roles for TMEM184B in long-term maintenance of pruriceptors.

In summary, we show that TMEM184B activity critically affects the development of pruriceptive neurons in mouse DRG and that this effect is likely due to its ability to induce components of Wnt signaling during neurogenesis. Our data illuminates a new key regulatory step in the processes controlling the establishment of diversity in the somatosensory system.

## Online Methods

### Animal Models

All animal treatment was approved by the Institutional Animal Care and Use Committee at the University of Arizona (protocol # 17-216). *Tmem184b* gene-trap mice have been described previously (Bhattacharya et al., 2016). Mice were bred to *Sst*<sup>Cre</sup> and Rosa-Flox-stop-Flox-tdTomato (also called Ai9) (lines 013044 and 007909, Jackson Laboratory, Bar Harbor, ME) for histological quantification of the C2 population. Only heterozygous *Sst*<sup>Cre</sup> mice were used for experiments due to the possible disruption of normal somatostatin expression in homozygous Cre mice.

### RNA sequencing

Total RNA was isolated from adult DRG from 6-month old mutant and wild-type mice (4 per genotype, mixed male and female groups) using the RNeasy Micro kit (Ambion). All DRGs were pooled for each sample to obtain enough RNA for analysis. Following total RNA extraction, samples were ethanol precipitated to increase purity. Library preparation and sequencing was performed at the Washington University Genome Technology Access Center (GTAC). Data were analyzed using Salmon and DeSeq2 (on our servers or with Galaxy, [www.usegalaxy.org](http://www.usegalaxy.org)). Volcano plots were generated in RStudio; heatmaps of genes for which adjusted P values were less than 0.05 were created using Cluster 3.0 and Java Treeview. To create heatmaps of normalized counts, hierarchical clustering was used in Cluster3.0 to arrange genes by expression similarity. For embryonic DRG analysis, total RNA was isolated using TRIzol and library preparation and sequencing was performed by Novogene; identical analysis methods were used. For bioinformatics analysis, we used Panther's over-representation analysis of biological processes (complete) (<http://www.pantherdb.org/>) as well as Enrichr ([www.enrichr.com](http://www.enrichr.com)). Fold enrichment, calculated as the number of statistically significantly expressed genes from the input dataset divided by the number of genes expected from the

entire mouse reference genome. Expected genes in a GO category calculated by applying the proportion of all genes in reference genome associated with a GO category to the number of genes in input dataset. Significance calculated by Fisher's exact test with a BHM FDR  $\leq 0.05$ .

### **Cytokine Injections and Behavior Analysis**

Mice were at least 8 weeks old at the time of injection. For itch experiments, both males and females of approximately equal quantities were used and data were pooled. Littermate controls were used, and videos were captured early in the morning to minimize mice falling asleep during videotaping. Mice were acclimated to behavioral chambers (red Rat Retreats, Bioserv) for one hour, removed from the chamber briefly for injections of either IL-31 (Peprotech, 3 nmol in 10 microliters of PBS for cheek injections or 300  $\mu$ M for nape injections, depending on experiment), chloroquine (concentration), or 0.9% saline alone, and returned to the chamber, at which time videotaping began. Analysis was done blinded to genotype and injected substance. Scratching bouts were tallied for 30 minutes post-injection. Tail flick, hot plate, and Von Frey testing methods have been previously described. (Bannon and Malmberg, 2007; Chaplan et al., 1994; Hargreaves et al., 1988) For pain and mechanical threshold testing, the experimenter was blinded to genotype, and males and females were separated during analysis.

### **AAV Injection**

Custom AAV9 was built and titered by Vector Biolabs. Viruses were intrathecally injected (10ul,  $2.0 \times 10^6$  virus particles/mL) at 8 to 9 weeks of age. Each mouse received intradermal (i.d.) saline injections 3 weeks after AAV delivery, and one week later received i.d. IL-31 injections. One Tmem184b mutant mouse with  $\sim 10x$  average scratching behavior to both saline and IL-31 was treated as an outlier and removed from our analysis.

### **DRG Immunohistochemistry and Image Analysis**

Isolated ganglia or spinal cords were fixed with 4% paraformaldehyde for 1 hour, immersed in 30% sucrose overnight (4°C), and embedded in OCT cryo-compound (Tissue-Tek® O.C.T.) using isopentane cooled with dry ice. Spinal cords were dissected into segments containing two

spinal segments (e.g. cervical 1 and 2). DRG cryosections (14  $\mu\text{m}$  thickness) or spinal cord sections (20  $\mu\text{m}$  thickness) were mounted onto charged microscope slides. Following washes in PBST and 1 hour of blocking in 5% goat serum in PBST, sections were incubated overnight at 4°C with rabbit NeuN (1:250, Proteintech), or for 1 hour with Alexa Fluor® 488 Mouse anti- $\beta$ -Tubulin, Class III (BD Pharmingen). Secondary antibody for NeuN was goat anti-rabbit Alexa Fluor 633 (Thermo Fisher). Sections were mounted in Vectashield (Vector Biolabs). Spinal cords were imaged with a ZEISS AxioZoom V16 Fluorescent Microscope. DRGs were imaged using a ZEISS Axio Observer Z1 or LSM880 inverted confocal microscope. For DRG counting, only neurons with a visible NeuN-positive nucleus in the section were counted. For each genotype, n = 5 mice. For each mouse,  $\geq 800$  neurons were counted.

### **Neuronal Culture**

For adult neurons, ganglia from all spinal levels were pooled in DMEM on ice, followed by digestion with Liberase TM (Roche) and 0.05% Trypsin (Gibco). Neurons were dissociated with a P1000 pipette tip, spotted in dense culture spots (20 $\mu\text{L}$ ) on poly-D-lysine (Sigma) and laminin coated chambered coverglass (Nunc) or 100mm glass coverslips, and grown overnight in Dulbecco's Modified Eagle Medium (Gibco) with 10% fetal bovine serum (Atlas Biologicals) and Penicillin/Streptomycin (Gibco). For embryonic DRG culture, ganglia were dissociated with Trypsin, triturated with a P1000 pipette tip, and plated in 5-10  $\mu\text{L}$  spots in a 24-well dish previously coated with poly-D-lysine and laminin. Media contained B27 (Gibco), 5-fluoro-deoxy-uridine (FDU) and nerve growth factor (NGF) (Invitrogen). Half of the media volume was exchanged every 5 days until cells were collected for analysis.

### **Calcium Imaging**

Adult DRG neurons were imaged either with Fluo-4 dye on a Zeiss Observer Z1 microscope, or with Fura-2 dye on an Olympus BXW microscope under a 10X immersion objective lens with a filter wheel and Hamamatsu camera, each with a frame rate of one image/3 sec. Fluorescence videos were acquired via Zeiss or HCLImage Software, processed and analyzed using MATLAB,

and RStudio for quantification of fluorescent responses. We used a custom-written R script to identify neurons via responses to high potassium in each experiment. Responses to individual agonists were determined manually for all neurons. Each agonist was evaluated using cultures from at least 3 mice, and most agonist-genotype combinations have >1000 neurons analyzed (minimum 659, maximum 2333). Coverslips with extensive motion or other artifacts were excluded from analysis.

### **Statistics**

All statistical analysis was performed in Graphpad Prism. Where applicable for multiple test corrections, all False-Discovery Rates determined with Benjamini-Hochberg Method (BHM); thresholds set at  $(FDR) \leq 0.05$ . For all figures, asterisks indicate  $p < 0.05$  (\*),  $p < 0.01$  (\*\*),  $p < 0.001$  (\*\*\*), or  $p < 0.0001$  (\*\*\*\*). For calcium imaging, binomial response counts were analyzed using two-sided Chi-square tests. In all experiments, independent samples were measured.

### **Data availability**

The data sets generated and analyzed in the current study will be deposited at NCBI GEO upon publication and linked to this manuscript.

### **Code availability**

All custom-written code in R and MATLAB for calcium imaging analysis will be made available on GitHub upon publication at [https://github.com/martharcb/Fluo4\\_R.git](https://github.com/martharcb/Fluo4_R.git).

### **Acknowledgements**

We would like to thank Dr. Aubin Moutal for assistance with adult DRG cultures and calcium imaging. This work was supported by the University of Arizona (Technology and Research Incentive Fund) and R01 NS105680 to M.R.C.B.

### **Author Contributions**

E.L. and M.B. designed the experiments. E.L. and M.B. performed RNAseq analysis and calcium imaging and analysis. T.C., J.F., E.L., C.M. and M.B. performed behavioral experiments. E.L., M.M., T.C, B.M., N.K., E.W., C.J., H.G. and M.B. analyzed behavior videos. T.L. performed intrathecal AAV injections. H.H. and R.K. supported experiments in their laboratories and offered guidance on the project. E.G.L. and M.R.C.B. wrote the manuscript.

### **Competing Interests Statement**

The authors declare no competing interests.



## References

- Acton, D., Ren, X., Di Costanzo, S., Dalet, A., Bourane, S., Bertocchi, I., Eva, C., and Goulding, M. (2019). Spinal Neuropeptide Y1 Receptor-Expressing Neurons Form an Essential Excitatory Pathway for Mechanical Itch. *Cell Rep.* **28**, 625-639.e6.
- Bannon, A.W., and Malmberg, A.B. (2007). Models of Nociception: Hot-Plate, Tail-Flick, and Formalin Tests in Rodents. In *Current Protocols in Neuroscience*, (John Wiley & Sons, Inc.), p.
- Bhattacharya, M.R.C., Geisler, S., Pittman, S.K., Doan, R.A., Weihl, C.C., Milbrandt, J., and DiAntonio, A. (2016). TMEM184b promotes axon degeneration and neuromuscular junction maintenance. *J. Neurosci.* **36**.
- Bourane, S., Duan, B., Koch, S.C., Dalet, A., Britz, O., Garcia-Campmany, L., Kim, E., Cheng, L., Ghosh, A., Ma, Q., et al. (2015). Gate control of mechanical itch by a subpopulation of spinal cord interneurons. *Science* **350**, 550–554.
- Cevikbas, F., Wang, X., Akiyama, T., Kempkes, C., Savinko, T., Antal, A., Kukova, G., Buhl, T., Ikoma, A., Buddenkotte, J., et al. (2014). A sensory neuron-expressed IL-31 receptor mediates T helper cell-dependent itch: Involvement of TRPV1 and TRPA1. *J. Allergy Clin. Immunol.* **133**, 448–460.
- Chaplan, S.R., Bach, F.W., Pogrel, J.W., Chung, J.M., and Yaksh, T.L. (1994). Quantitative assessment of tactile allodynia in the rat paw. *J. Neurosci. Methods* **53**, 55–63.
- Chiu, I.M., Barrett, L.B., Williams, E.K., Strohlic, D.E., Lee, S., Weyer, A.D., Lou, S., Bryman, G.S., Roberson, D.P., Ghasemlou, N., et al. (2014). Transcriptional profiling at whole population and single cell levels reveals somatosensory neuron molecular diversity. *Elife* **3**.
- Dillon, S.R., Sprecher, C., Hammond, A., Bilsborough, J., Rosenfeld-Franklin, M., Presnell, S.R., Haugen, H.S., Maurer, M., Harder, B., Johnston, J., et al. (2004). Interleukin 31, a cytokine produced by activated T cells, induces dermatitis in mice. *Nat. Immunol.* **5**, 752–760.
- Dong, X., and Dong, X. (2018). Peripheral and Central Mechanisms of Itch. *Neuron* **98**, 482–494.

Garcia-Morales, C., Liu, C.-H., Abu-Elmagd, M., Hajihosseini, M.K., and Wheeler, G.N. (2009). Frizzled-10 promotes sensory neuron development in *Xenopus* embryos. *Dev. Biol.* 335, 143–155.

Hargreaves, K., Dubner, R., Brown, F., Flores, C., and Joris, J. (1988). A new and sensitive method for measuring thermal nociception in cutaneous hyperalgesia. *Pain* 32, 77–88.

Huang, C., Lu, F., Li, P., Cao, C., and Liu, Z. (2017). Tlx3 Function in the Dorsal Root Ganglion is Pivotal to Itch and Pain Sensations. *Front. Mol. Neurosci.* 10, 205.

Huang, J., Polgár, E., Solinski, H.J., Mishra, S.K., Tseng, P.-Y., Iwagaki, N., Boyle, K.A., Dickie, A.C., Kriegbaum, M.C., Wildner, H., et al. (2018). Circuit dissection of the role of somatostatin in itch and pain. *Nat. Neurosci.* 21, 707–716.

Kondo, T., Matsuoka, A.J., Shimomura, A., Koehler, K.R., Chan, R.J., Miller, J.M., Srour, E.F., and Hashino, E. (2011). Wnt signaling promotes neuronal differentiation from mesenchymal stem cells through activation of Tlx3. *Stem Cells* 29, 836–846.

Lallemend, F., and Ernfors, P. (2012). Molecular interactions underlying the specification of sensory neurons. *Trends Neurosci.* 35, 373–381.

Lee, H.Y., Kléber, M., Hari, L., Brault, V., Suter, U., Taketo, M.M., Kemler, R., and Sommer, L. (2004). Instructive Role of Wnt/ $\beta$ -Catenin in Sensory Fate Specification in Neural Crest Stem Cells. *Science* (80-. ). 303, 1020–1023.

Li, C.-L., Li, K.-C., Wu, D., Chen, Y., Luo, H., Zhao, J.-R., Wang, S.-S., Sun, M.-M., Lu, Y.-J., Zhong, Y.-Q., et al. (2016a). Somatosensory neuron types identified by high-coverage single-cell RNA-sequencing and functional heterogeneity. *Cell Res.* 26, 83–102.

Li, C.-L., Li, K.-C., Wu, D., Chen, Y., Luo, H., Zhao, J.-R., Wang, S.-S., Sun, M.-M., Lu, Y.-J., Zhong, Y.-Q., et al. (2016b). Somatosensory neuron types identified by high-coverage single-cell RNA-sequencing and functional heterogeneity. *Cell Res.* 26, 83–102.

Liu, Q., Tang, Z., Surdenikova, L., Kim, S., Patel, K.N., Kim, A., Ru, F., Guan, Y., Weng, H.-J., Geng, Y., et al. (2009). Sensory neuron-specific GPCR Mrgprs are itch receptors mediating

chloroquine-induced pruritus. *Cell* **139**, 1353–1365.

Lopes, C., Liu, Z., Xu, Y., and Ma, Q. (2012). Tlx3 and Runx1 act in combination to coordinate the development of a cohort of nociceptors, thermoceptors, and pruriceptors. *J. Neurosci.* **32**, 9706–9715.

Oetjen, L.K., Mack, M.R., Feng, J., Whelan, T.M., Niu, H., Guo, C.J., Chen, S., Trier, A.M., Xu, A.Z., Tripathi, S. V, et al. (2017). Sensory Neurons Co-opt Classical Immune Signaling Pathways to Mediate Chronic Itch. *Cell* **171**, 217-228.e13.

Pagani, M., Albisetti, G.W., Sivakumar, N., Wildner, H., Santello, M., Johannssen, H.C., and Zeilhofer, H.U. (2019). How Gastrin-Releasing Peptide Opens the Spinal Gate for Itch. *Neuron* **103**, 102-117.e5.

Pan, H., Fatima, M., Li, A., Lee, H., Cai, W., Horwitz, L., Hor, C.C., Zaher, N., Cin, M., Slade, H., et al. (2019). Identification of a Spinal Circuit for Mechanical and Persistent Spontaneous Itch. *Neuron* **103**, 1135-1149.e6.

Raisa Eng, S., Gratwick, K., Rhee, J.M., Fedtsova, N., Gan, L., and Turner, E.E. (2001). Defects in sensory axon growth precede neuronal death in Brn3a-deficient mice. *J. Neurosci.* **21**, 541–549.

Sharma, N., Flaherty, K., Lezgiyeva, K., Wagner, D.E., Klein, A.M., and Ginty, D.D. (2020). The emergence of transcriptional identity in somatosensory neurons. *Nature* **577**, 392–398.

Shen, C., Li, L., Zhao, K., Bai, L., Wang, A., Shu, X., Xiao, Y., Zhang, J., Zhang, K., Hui, T., et al. (2018). Motoneuron Wnts regulate neuromuscular junction development. *Elife* **7**.

Solinski, H.J., Kriegbaum, M.C., Tseng, P.-Y., Earnest, T.W., Gu, X., Barik, A., Chesler, A.T., and Hoon, M.A. (2019). Nppb Neurons Are Sensors of Mast Cell-Induced Itch. *Cell Rep.* **26**, 3561-3573.e4.

Usoskin, D., Furlan, A., Islam, S., Abdo, H., Lönnerberg, P., Lou, D., Hjerling-Leffler, J., Haeggström, J., Kharchenko, O., Kharchenko, P. V, et al. (2015). Unbiased classification of sensory neuron types by large-scale single-cell RNA sequencing. *Nat. Neurosci.* **18**, 145–153.

Wilson, S.R., Thé, L., Batia, L.M., Beattie, K., Katibah, G.E., McClain, S.P., Pellegrino, M., Estandian, D.M., and Bautista, D.M. (2013). The epithelial cell-derived atopic dermatitis cytokine TSLP activates neurons to induce itch. *Cell* *155*, 285–295.

Yee, D.C., Shlykov, M.A., Västermark, A., Reddy, V.S., Arora, S., Sun, E.I., Saier, M.H., and Jr. (2013). The transporter-opsin-G protein-coupled receptor (TOG) superfamily. *FEBS J.* *280*, 5780–5800.

Zheng, Y., Liu, P., Bai, L., Trimmer, J.S., Bean, B.P., and Ginty, D.D. (2019). Deep Sequencing of Somatosensory Neurons Reveals Molecular Determinants of Intrinsic Physiological Properties. *Neuron* *103*, 598-616.e7.

## Figure Legends

**Figure 1. TMEM184B Controls the Expression of Pruriceptive Markers.** (A) Volcano plot of RNA-sequencing data. Light blue, significantly differentially expressed genes (n = 381 genes) navy, most well-known itch-related differentially expressed genes (n = 24 genes); gray, non-differentially expressed genes (n = 12,550 genes). Benjamini-Hochberg Method-derived FDR;  $FDR \leq 0.05$ , dashed red line. (B) Heatmap showing aligned, variance-normalized samples (n = 4 per genotype), and differentially expressed genes identified using DESeq2 ( $FDR \leq 0.05$ , n = 405 genes) independently clustered by expression similarity. At right, the top section of the heatmap is expanded to show individual genes that are most strongly downregulated by loss of *Tmem184b*. (C) Venn diagram of a subset of downregulated genes showing their specific expression in subsets of nociceptors. (D) Over-represented Panther pathways ( $FDR \leq 0.05$ ) in downregulated genes.

**Figure 2. TMEM184B is required for itch, but not pain, responses.** (A) *Tmem184b*-mutant mice show reduced scratching to IL-31 injection. Data presented as mean  $\pm$  SD (n = 7,7,5,5 L to R;  $F(3,20) = 4.49$ ,  $p = 0.014$ , One-way ANOVA). (B) Chloroquine-induced scratching responses. Data presented as mean  $\pm$  SD (n = 11,12,6,5 L to R;  $F(3,20) = 2.57$ ,  $p = 0.073$ , One-Way ANOVA). (C) Hot plate analysis. Data presented as mean  $\pm$  SD (n = 13,13,9,14, L to R. Female:  $15.55 \pm 5.66$ ,  $17.78 \pm 6.02$ ;  $t = 0.973$ ,  $p = 0.3404$ ; Male:  $12.27 \pm 6.33$ ,  $13.31 \pm 5.95$ ,  $t = 0.400$ ,  $p = 0.694$ ). (D) Tail flick analysis. Data presented as mean  $\pm$  SD (n = 13,13,10,10, L to R. Female:  $5.96 \pm 3.59$ ,  $5.61 \pm 1.83$ ,  $t = 0.307$ ,  $p = 0.762$ ; Male:  $4.75 \pm 2.47$ ,  $5.03 \pm 1.80$ ,  $t = 0.298$ ,  $p = 0.769$ ). (E) Baseline mechanical thresholds. Data presented as mean  $\pm$  SD (n = 13,11,9,8, L to R).

R. Female:  $3.69 \pm 1.68$ ,  $3.91 \pm 1.37$ ,  $t = 0.342$ ,  $p = 0.735$ ; Male:  $3.75 \pm 1.09$ ,  $3.76 \pm 1.01$ ,  $t = 0.022$ ,  $p = 0.983$ ). For C-E,  $p$  values were calculated using two-tailed, unpaired  $t$ -tests.

**Figure 3. TMEM184B is required for normal numbers of NP3/C2 neurons.** (A) Adult DRG sections showing neurons labeled with NeuN (left) and Sst-Cre>Ai9 (middle) in wild type and *Tmem184b* mutant neurons. The merged image is shown at right. (B) Percent of neurons labeled with Sst-Cre>Ai9 in wild type and *Tmem184b*-mutant mice.  $n=5-6$  mice and  $\geq 800$  neurons analyzed per mouse. Data presented as mean  $\pm$  SD ( $7.20 \pm 2.00$ ,  $4.21 \pm 1.74$ ,  $t = 2.52$ ,  $p = 0.036$ , unpaired  $t$  test). (C-H) Normalized counts of individual genes from RNAseq analysis of E13, P0, and P10 mutant and wild type mouse dorsal root ganglia.  $n = 3-4$  mice per time-point and genotype. Asterisks indicate statistical significance as calculated by DESeq2 (Wald Test with  $FDR \leq 0.05$ ). Data presented as mean  $\pm$  SEM. (C) *Tmem184b* ( $q < 0.0001$  for both E13 and P0) (D) *Sst* ( $q = 0.0082$  for P0;  $q < 0.0001$  for P10). (E) *Il31ra* ( $q = 0.09$ ). (F) *Nppb* (not significant). (G) *Neurog1* ( $q < 0.0001$ ). (H) *Neurog2* ( $q < 0.0001$ ). (I) *Pou4f1* ( $q = 0.0034$ ;  $q < 0.0001$ ).

**Figure 4. Aberrant cellular responses to nociceptive and pruriceptive agonists in *Tmem184b*-mutant mice.** Total analyzed neurons and percent responders are shown for (A) Capsaicin ( $1\mu\text{M}$ ), a TRPV1 agonist, (B) AITC ( $200\mu\text{M}$ ), a TRPA1 agonist, (C)  $\beta$ -alanine ( $5\text{mM}$ ), an MRGPRD agonist, (D) CYM5442 ( $250\mu\text{M}$ ), an S1PR1 agonist, (E) LY344862 ( $2.5\mu\text{M}$ ), an HTR1F agonist, (F) IL-31 ( $1\mu\text{M}$ ), and (G) chloroquine (CQ,  $200\mu\text{M}$ ), an MRGPRA3 agonist. Data presented as binomial responses; proportions of positive responses as inlaid percentage. Statistical significance was calculated using two-tailed Chi-square analysis. (H) Average IL-31 response calculated from wild type (thick blue) and mutant (thick orange) neurons classified as

IL-31 responders. Wild type (n = 19) and mutant (n = 24) neurons cultured and imaged on the same day with the same solutions were averaged. Two individual neurons from each genotype contributing to the average trace are shown (faint blue, wild type; faint orange, mutant).

**Figure 5. In vivo re-expression of *Tmem184b* in adult mutant ganglia does not increase IL-31 responses.** (A) Schematic of the adult rescue experiment. (B) DRG from cervical regions of AAV-injected mice, showing successful virus infection and spread between C1-C10 (mCherry). (C) Spinal cord expression of mCherry in both incoming DRG processes (left) and in grey matter (right). (D) Wild type and *Tmem184b* mutant scratch responses, sorted by AAV type and agonist (IL-31, filled squares; saline, open circles). n = 8,7 animals, L-R. Analysis by two-way ANOVA with Tukey's correction for multiple comparisons. P values in wild type: mCherry saline vs IL-31, p = 0.0005; IL-31 mCherry vs *Tmem184b* virus, p = 0.0024.

**Figure 6. TMEM184B controls expression of Wnt signaling components in embryonic DRG neurons.** (A) Schematic of the experimental design. Samples from dissociated DRG neurons (1 and 2, n = 4 per group) and DIV 14 neurons (3-5, n = 5 per group) were collected for RNAseq analysis. (B-C), Volcano plots showing (B) DIV14 *Tmem184b*-mutant vs DIV14 WT and (C) DIV14 rescue vs DIV14 mutant transcript expression. Red horizontal line is threshold for significance (FDR ≤ 0.05). Red, downregulated genes with  $\log_2FC \leq -0.5$ ; blue,  $-0.5 < \log_2FC < 0.5$ ; green, upregulated genes with  $\log_2FC \geq 0.5$ . (D) Genes both downregulated in DIV14 mutant eDRGs (B, red) and upregulated in rescued DIV14 mutant eDRGs (C, green) were analyzed using Panther gene ontology over-representation analysis. GO Biological Processes with ≥ 5-fold enrichment are shown.

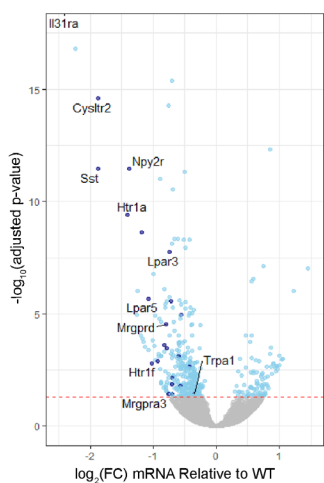
**Supplemental Figure 1. Genes with known roles in development or maturation of sensory neurons are differentially affected by *Tmem184b* loss.** (A) Cysteinyl leukotriene receptor 2 (*Cysltr2*). (B) Serotonin receptor 1F (*Htr1f*). (C) MAS-related GPR, member A3 (*Mrgpra3*). (D-F) RUNX family transcription factors 1, 2, and 3 (*Runx1*, *Runx2*, *Runx3*;  $q < 0.0001$ ). (G-I) Neurotrophic receptor tyrosine kinase 1, 2, and 3 (*Ntrk1* (TrkA), *Ntrk2* (TrkB), *Ntrk3* (TrkC)). (J-L) Mitogen-activated protein kinase 8-10 (*Mapk8* (JNK1), *Mapk9* (JNK2,  $q = 0.007$ ), *Mapk10* (JNK3,  $q = 0.0005$ )). (M)  $\beta$ -catenin (*Ctnnb1*,  $q < 0.0001$ ). (N) Glycogen synthase kinase 3 beta (*Gsk3 $\beta$* ). (O) T cell leukemia, homeobox 3 (*Tlx3*;  $q = 0.021$  for E13,  $q = 0.041$  for P0,  $q = 0.029$  for P10).

**Supplemental Figure 2. Fold enrichment of GO biological processes over-represented in the set of genes negatively regulated by *Tmem184b* expression.** All over-represented Panther Gene Ontology biological processes with statistically significant fold enrichment. Fold enrichment, the strength of over- or under-representation, calculated as the number of statistically significantly expressed genes from the input dataset divided by the number of genes expected from the entire reference genome. Expected genes in a GO category calculated by applying the proportion of all genes in reference genome associated with GO category to the number of genes in input dataset. Significance calculated by Fisher's exact test with a BHM  $FDR \leq 0.05$ .

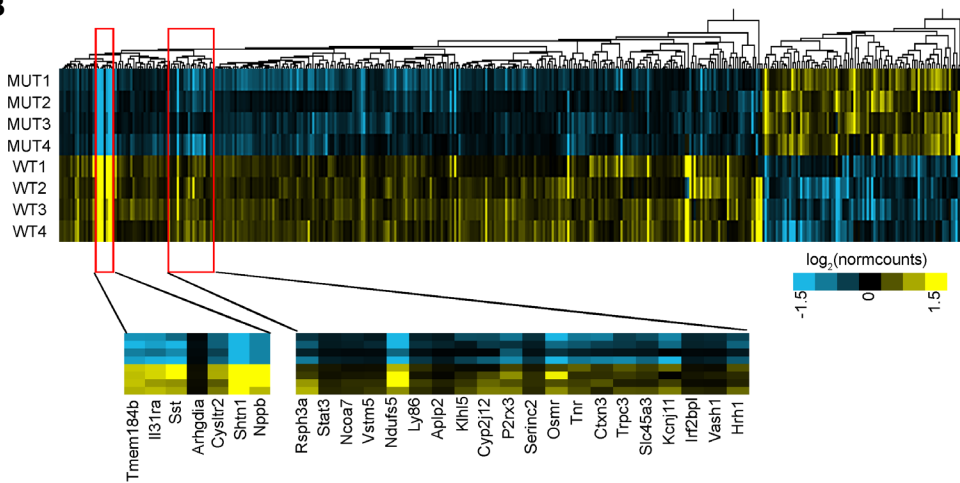


**Figure 1. Tmem184b Controls the Expression of Pruriceptive Markers.**

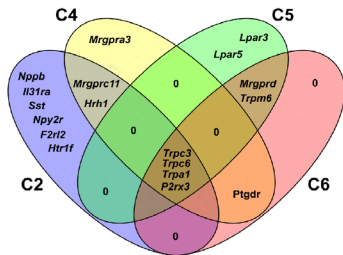
**A**



**B**



**C**



**D**

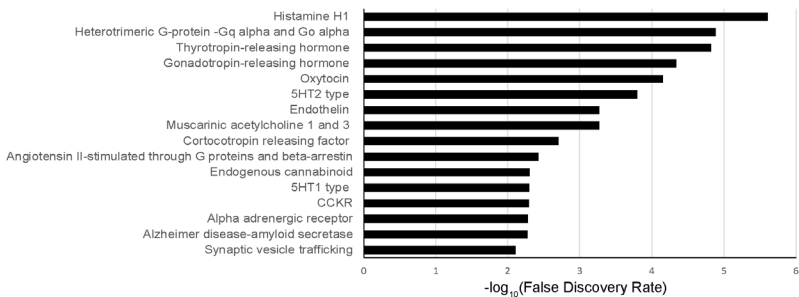


**Figure 2. Tmem184b is required for itch, but not pain, responses.**

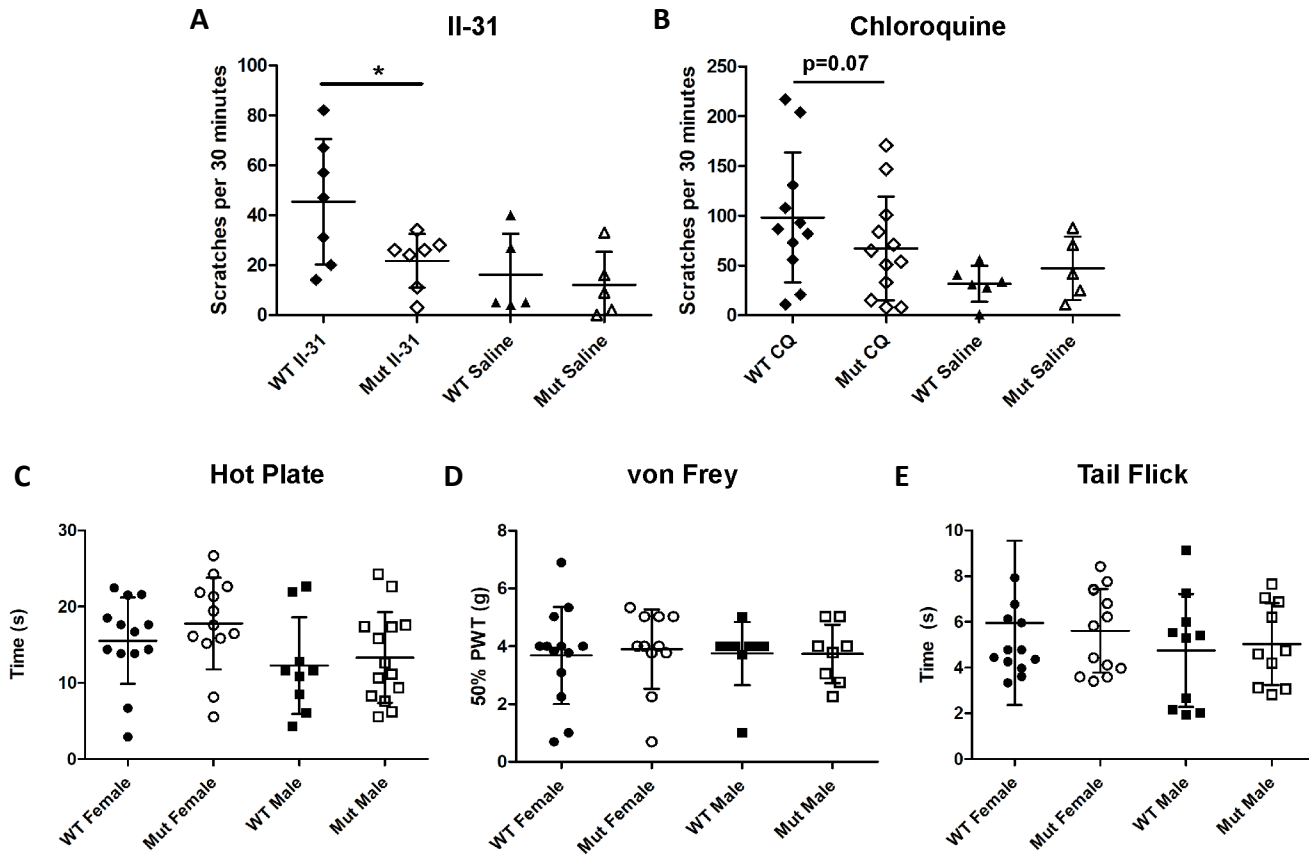


**Figure 3. Tmem184b is required for normal numbers of NP3/C2 neurons.**

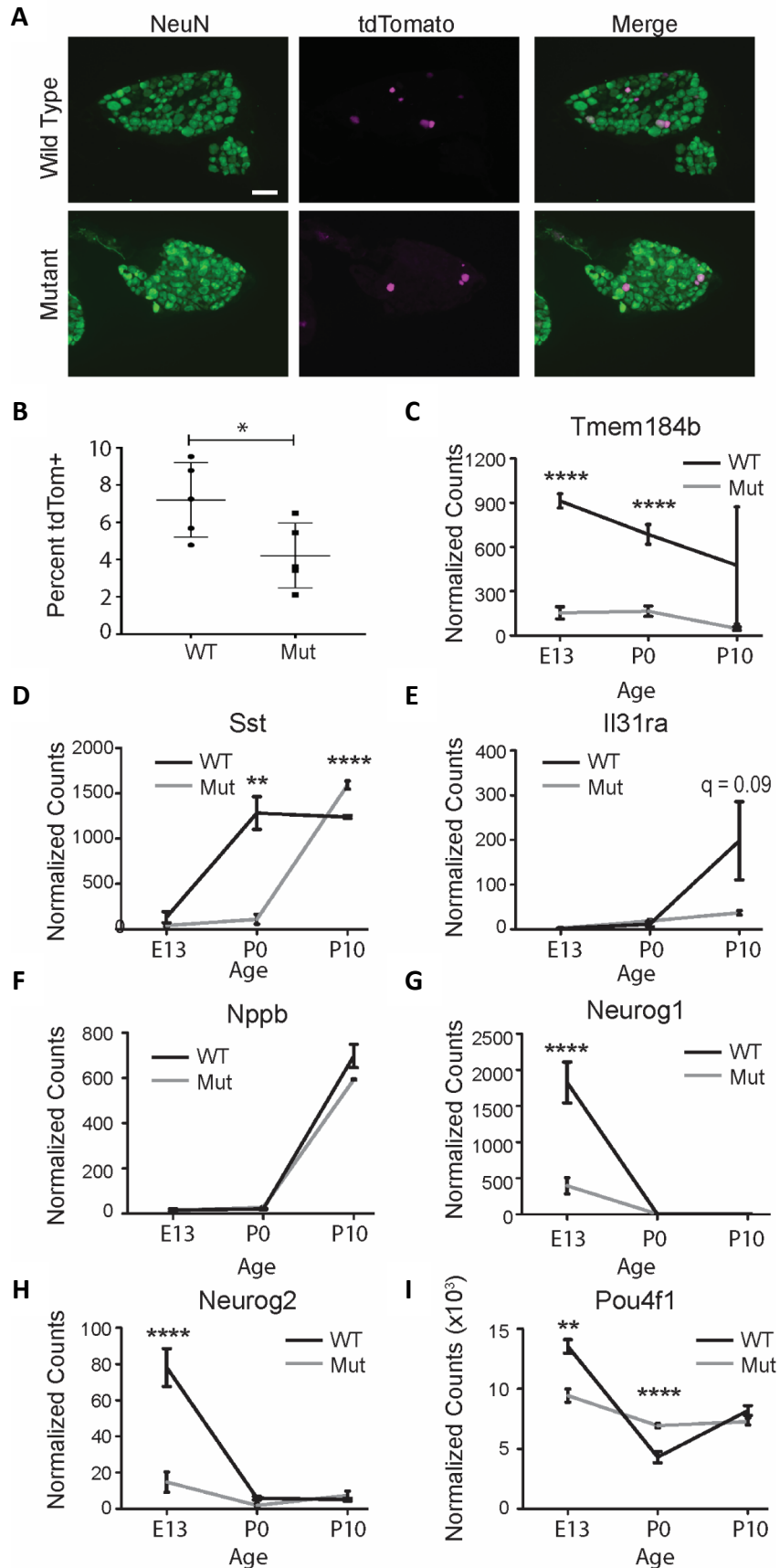


**Figure 4. Aberrant cellular responses to nociceptive and pruriceptive agonists in Tmem184b-mutant mice.**

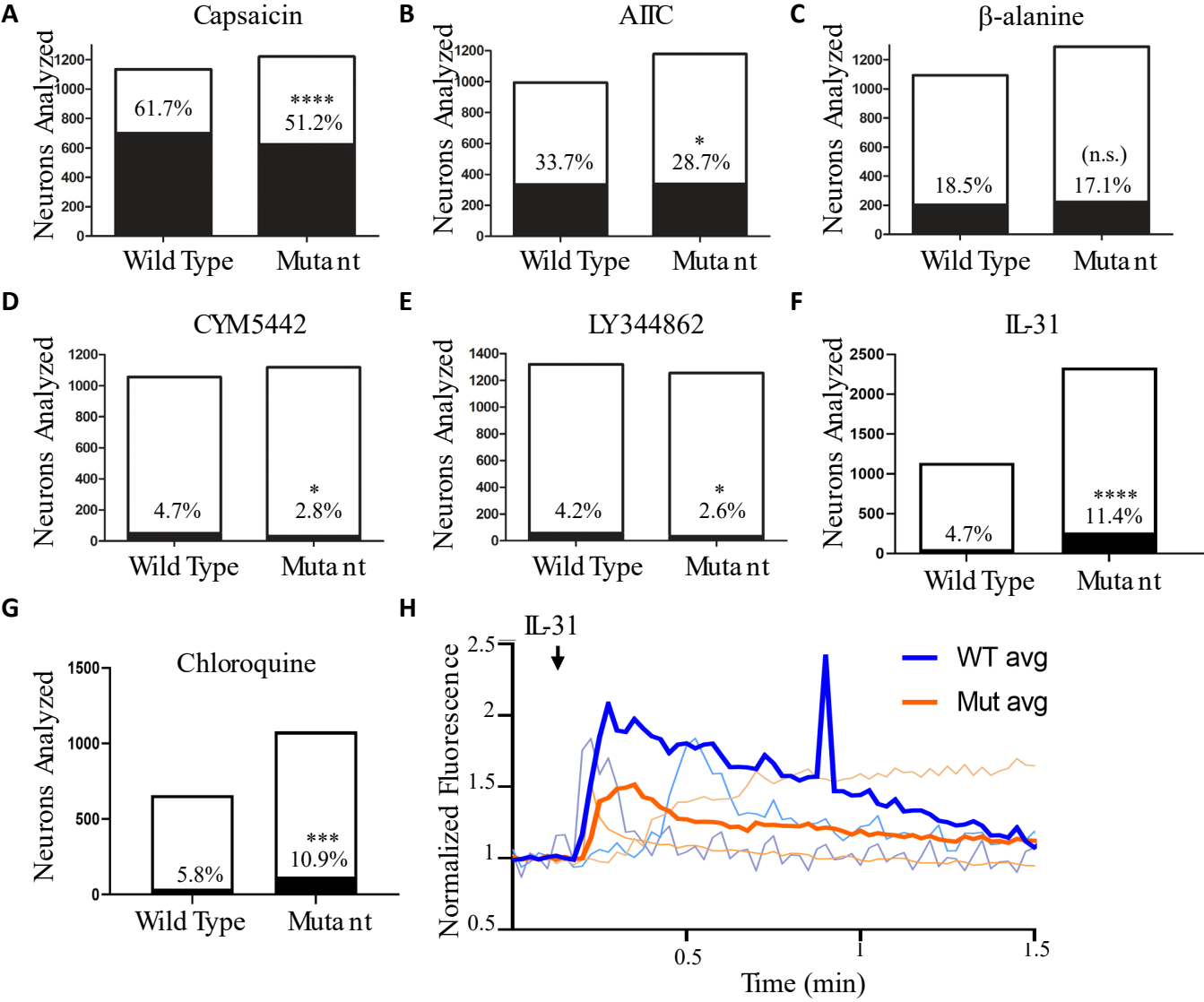


# Figure 5. In vivo re-expression of Tmem184b in adult mutant ganglia does not increase IL-31 responses.

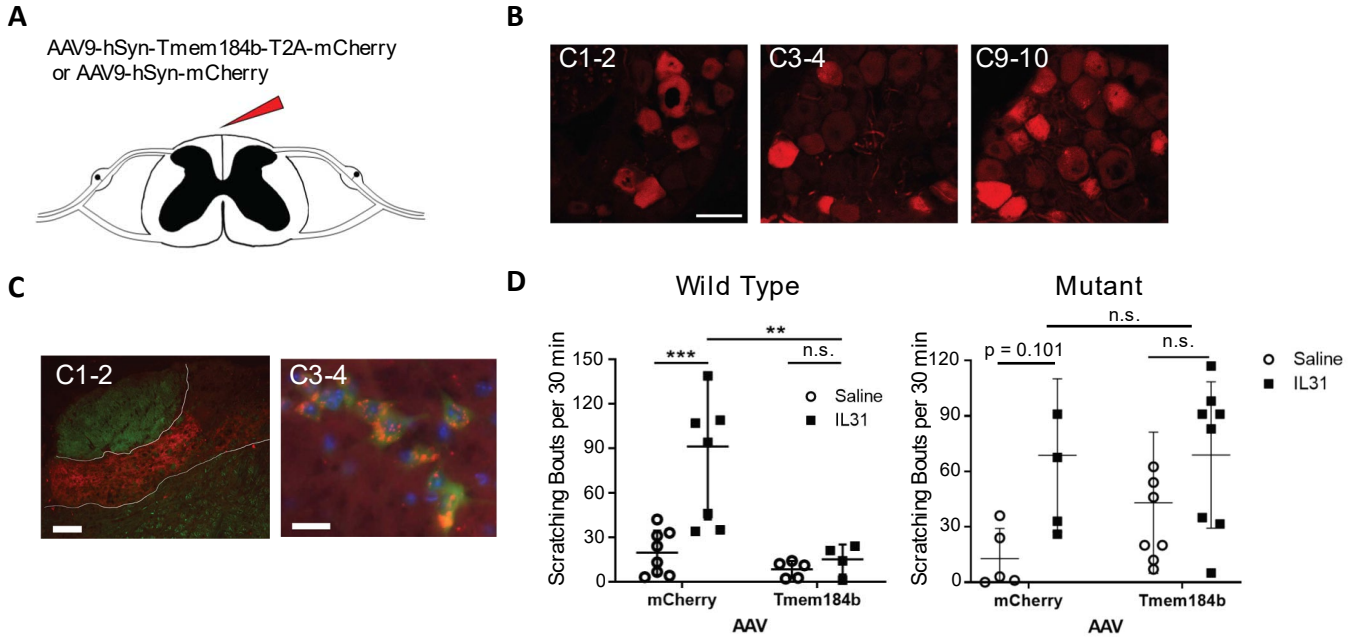
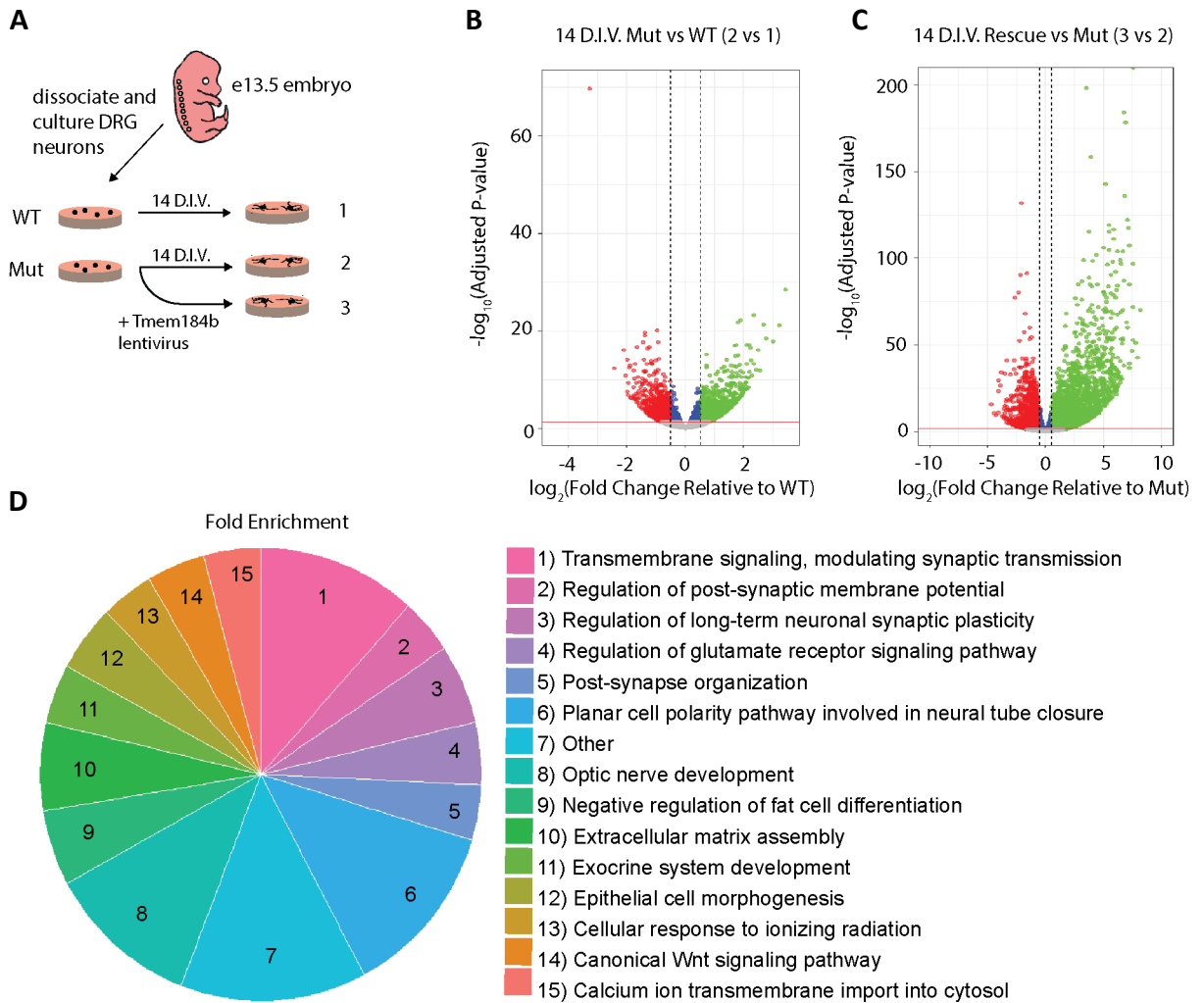
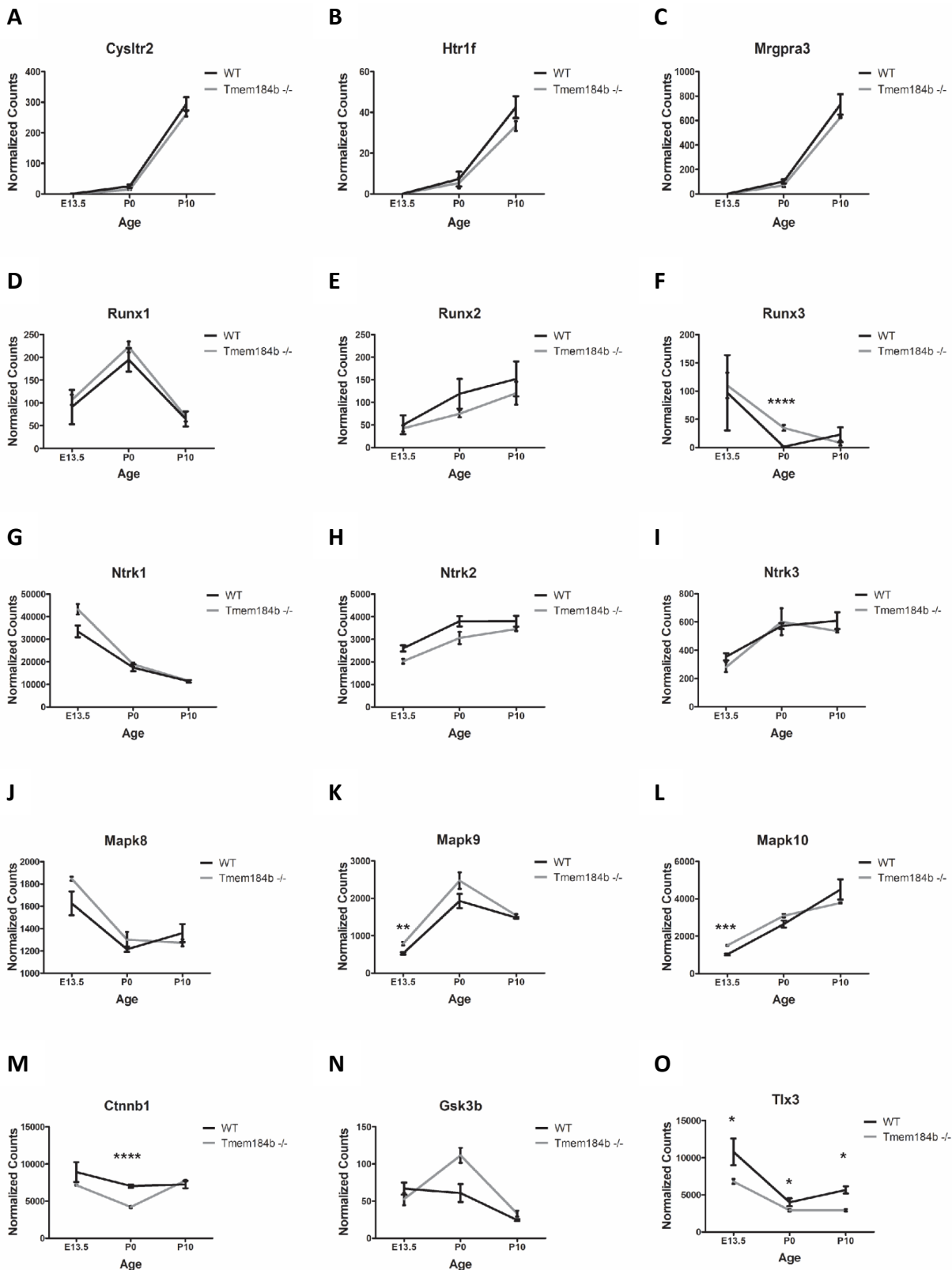


**Figure 6. Tmem184b controls expression of Wnt signaling components in embryonic DRG neurons.**



# Supplemental Figure 1. Genes with known roles in development or maturation of sensory neurons are differentially affected by *Tmem184b* loss.



## Supplemental Figure 2. Fold enrichment of GO biological processes over-represented in the set of genes negatively regulated by Tmem184b expression.

A

